Subtle role of counteranions in molecular construction: Structures and properties of novel Cu(II) coordination complexes with bis-(1-benzoimidazolymethylene)-(2,5-thiadiazoly)-disulfide

Yaru Liu [a,b], Jinpeng Li [a], Hongwei Hou [a,*], Yaoting Fan [a]

[a] Department of Chemistry, Zhengzhou University, Henan 450052, PR China
[b] School of Science, North University of China, Taiyuan 030051, PR China

ARTICLE INFO

ABSTRACT

The direct self-assembly of bis-(1-benzoimidazolymethylene)-(2,5-thiadiazoly)-disulfide (L) with $CuSO_4$, $Cu(NO_3)_2$ and $CuCl_2$ affords three novel supramolecular complexes: 1-D ladder-like chain complex $\{[Cu(SO_4)(L)] \cdot (CH_3OH)\}_n$ (**1**), dimer complexes $\{[Cu(L)(CH_3O)]_2(NO_3)_2\} \cdot 2H_2O$ (**2**) and $[Cu(L)(Cl)(N_3)]_2 \cdot 2\text{-}CH_3OH$ (**3**). The nature of the anions is the underlying reason behind the differences in the structures of this series of complexes. Furthermore, utilizing the coordinatively unsaturated complexes **2** and **3** as precursor complexes, two new derivative complexes $[Cu(L)(NCS)(CH_3O)]_2 \cdot 2CH_3OH$ (**2A**) and $[Cu(L)(ClO_4)(N_3)]_2 \cdot 2CH_3OH$ (**3A**) are obtained by the addition and exchange reactions of complexes **2** and **3** with anions. X-ray crystallographic analysis shows that the two derivatives retain the skeletons of their precursor complexes, and the anions with the stronger coordination capacity only bind to the active position of precursor complexes. In addition, different from the obvious effects on the structures in the direct self-assembly of the metal and ligand, the change of counteranions has no great impact on the structures in the anion exchange reactions. We also study the catalytic activities of the complexes **2**, **2A**, **3**, and **3A**, which have similar skeletons, for the oxidative coupling polymerization of 2,6-dimethylphenol (DMP). And we find that the introductions of different coordination counterions produce significant impacts on the catalytic properties of these complexes.

1. Introduction

Over the past several decades, the rational design and preparation of metallosupramolecular complexes have attracted intense interest for their unfamiliar architectures and potential applications [1–13]. Various kinds of novel supramolecular architectures have been successfully built by the rational combination of predesigned organic ligands containing appropriate coordination sites and elaborately choosing metal ions with definite coordination geometry [14–18]. However, in many cases, the structures of the resulting complexes are still hard to be predicted because the self-assembly progress is highly influenced by several factors, such as counterions, temperature and solvent, besides the metal/ligand nature [19–22]. In order to more precisely synthesize target complexes with desired structures and properties, it is necessary to systematically understand the influence of these subtle factors.

Recently, we have paid attention to the role of the counteranions upon the supramolecular architectures. To accurately gain information about the counteranions upon the structures and

properties, what need most of all is to overcome interference from other factors in the self-assemble progress. For the direct self-assembly of the metal and ligand, the simplest and most effective method is to design and synthesize complexes using the same building block, same metal center, and same experimental conditions and varying only the counteranions at a time. Besides the above direct self-assembly method, the coordination capability of counteranions can be also explored by anion exchange reactions of complexes. In theory, the coordinatively unsaturated complexes or complexes with weak coordination anions should be able to show wonderful reactivities in the presence of anions with the stronger coordination capacity [23–25]. So they can be desired to undergo the anion addition or exchange reactions, and to synthesize further a diverse set of reaction products. By comparing the differences of structures between the precursor complexes and new derivative complexes, the effect of the counteranions can be facilely explained in the self-assemble progress.

On the basis of the above considerations, we design and synthesize a new benzimidazole-based ligand bis-(1-benzoimidazolymethylene)-(2,5-thiadiazoly)-disulfide (L) and further obtain three novel copper complexes **1**, **2**, and **3** by the direct self-assembly. In addition, we utilize the coordinatively unsaturated complexes

---

* Corresponding author.
  E-mail address: houhongw@zzu.edu.cn (H. Hou).

2 and **3** as precursor complexes and synthesize two new derivative complexes **2A** and **3A** by the anion addition and exchange reactions. Then, we discuss the roles of counterions in the formation progresses of the series of complexes by analyzing the structures of these complexes. Finally, for the purpose of exploring the influence of counterions on the properties of complexes, we study the catalytic activities of the compounds **2**, **2A**, **3**, and **3A**, which have similar structure skeletons, for the oxidative coupling polymerization of 2,6-dimethylphenol (DMP).

2. Results and discussion

2.1. Synthesis of the complexes

As an excellent reaction prosoma, benzimidazole group is often used to construct multifunctional benzimidazole-based ligands with various configurations [26–30]. Herein, we design and synthesize a new benzimidazole-based bridging ligand bis-(1-benzoimidazolymethylene)-(2,5-thiadiazoly)-disulfide (L). L is selected for the following reasons: first, the versatile coordination modes and strong coordination capacity of the benzimidazole and 2,5-thiadiazoly groups make the self-assembly of crystal engineering easily available; second, due to the big steric hindrance of the benzimidazole and 2,5-thiadiazoly groups in L, the flexible ligand with multi-coordination sites tends to form low dimensional complexes via reacting with metal salts, and show wonderful reactivities in the presence of anions with the stronger coordination capacity. Using L as the main ligand, three novel copper complexes $\{[Cu(SO_4)(L)](CH_3OH)\}_n$ (**1**), $\{[Cu(L)(CH_3O)]_2(NO_3)_2\} \cdot 2H_2O$ (**2**) and $[Cu(L)(Cl)(N_3)]_2 \cdot 2CH_3OH$ (**3**) are obtained by the direct self-assembly of L and corresponding copper salts and subsidiary anions. In addition, the coordinatively unsaturated complexes **2**, **3** show wonderful reactivities in the presence of anions with the strong coordination capacity. When we utilize **2** as a precursor, $[Cu(L)(NCS)(CH_3O)]_2 \cdot 2CH_3OH$ (**2A**) is obtained by an anion addi-

tion process. $[Cu(L)(ClO_4)(N_3)]_2 \cdot 2CH_3OH$ (**3A**) is the addition and exchange reaction product of **3** with terminal Cl^- groups and $Cu(ClO_4)_2$ (Scheme 1).

2.2. Crystal structure of $\{[Cu(SO_4)(L)]\cdot(H_2O)\}_n$ (**1**)

Crystallographic analysis reveals that **1** crystallizes in the triclinic space group $P\bar{1}$ and exhibits a 1-D double-chain structure. Each Cu(II) ion is located in a tetragonal-pyramidal environment (Fig. 1). The basal sites of the coordination sphere are made up of two N-donor atoms from different L, two oxygen atoms from one coordinated SO_4^{2-} ion with the in-plane Cu–N distances being 1.986(4) and 1.959(3) Å and Cu–O distances being 1.994(3) and 2.000(3) Å (the mean deviation from plane of 0.0163 Å). One oxygen atom from another coordinated SO_4^{2-} ion, which lays 3.502 Å up the basal plane, occupies the apical position with a significantly longer Cu–O distance of 2.258(3) Å, showing the considerable Jahn–Teller distortion. Each sulfate anion binds to two Cu(II) ions in both the chelating and bridging fashions. The bond angles around Cu(II) ion vary from 71.06(13)° to 162.46(14)°. The L is twisted with the torsion angles of 63.6(4)° and 66.8(3)° for C9–S2–C8–N2 and C10–S4–C11–N5, respectively, and the dihedral angle between two benzimidazole rings is 109.3°. The two twisted L and two sulfate anions join four Cu(II) ions resulting in a 36-membered tetranuclear macrocycle. The Cu···Cu distance spanned by a pair of SO_4^{2-} ions is 4.471 Å and the Cu···Cu distance spanned by a pair of L ligand is 9.757 Å. These tetranuclear macrocycles as building blocks are repeatedly arranged through O → Cu (O–Cu 2.258 Å) coordinating interaction to generate an infinite double chain with a ladder-like profile (the rails consist of $\{Cu(L)\}_n$ chains, with the sulfate groups acting as the rungs). Such chains were further assembled by the weak S···S interactions (3.530 Å) involving the S atoms from the triazole moiety to form an infinite 2-D supramolecular network. These weak but significant intermolecular interactions stabilize the molecular structure in the crystal engineering.
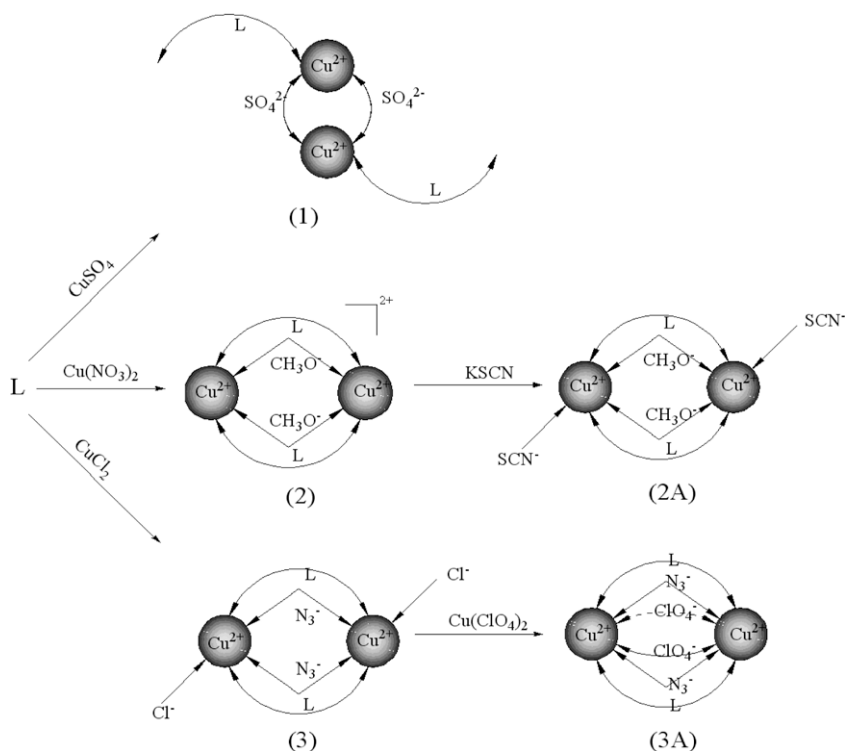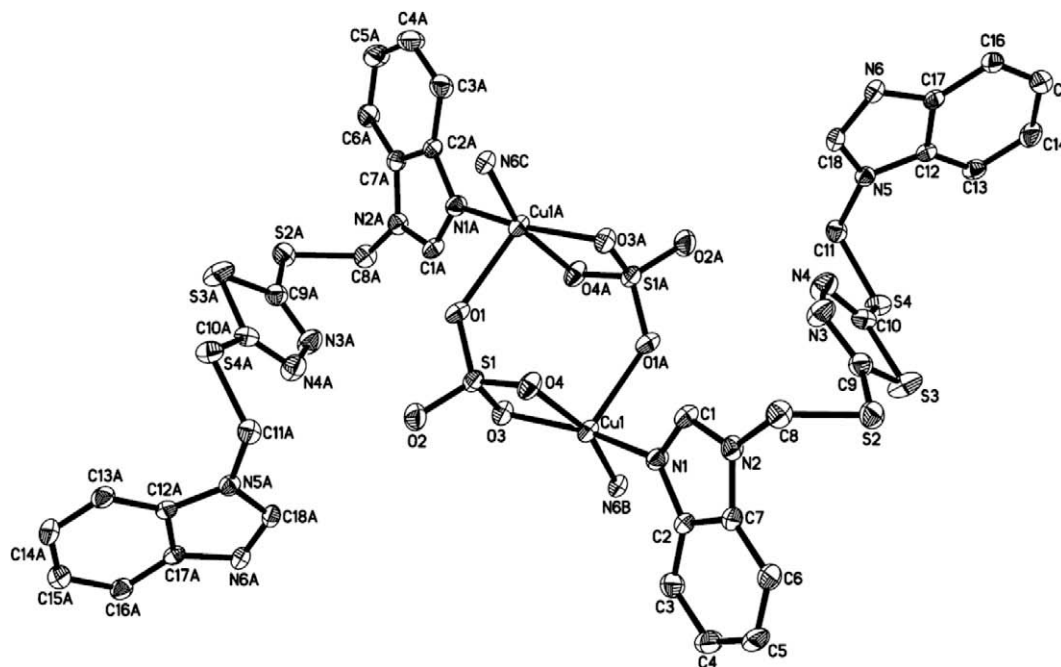

Scheme 1.

Fig. 1. ORTEP structure with 30% thermal ellipsoid probability for complex **1**.

2.3. Crystal structures of {[Cu(L)(CH₃O)]₂(NO₃)₂} · 2H₂O (2)

The structure analysis by X-ray diffraction demonstrates that the structure of **2** consists of cationic binuclear entities [Cu(L)(CH₃O)]₂²⁺, non-coordinated nitrate anions and methanol molecules as packing solvent (Fig. 2). This molecule crystallizes in the space group $P\bar{1}$. In each centrosymmetric [Cu(L)(CH₃O)]₂²⁺, two L acts as bridging ligands, bonding to separate Cu(II) centers through nitrogen atoms from benzimidazole groups. The distances of Cu1–N1 and Cu1–N6A are 1.945(5) and 2.022(5) Å, respectively. The torsion angles of C10–S3–C11–N5 and C9–S1–C8–N2 are −78.71 and 86.60°, respectively, and the dihedral angle between two benzimidazole rings is 62°. Meantime, the two symmetrical

Cu(II) centers are also bridged by two methoxy groups, leading to a planar dimeric [Cu₂O₂] core. The bond lengths of Cu(1)–O are 1.885(4) and 1.925(4) Å, respectively. And the Cu1···Cu1A separation is 2.849 Å.

In this complex, a two-dimensional interpenetrating diamond-oid network is constructed via the host molecule with the uncoordinated guest NO₃⁻ ion. Different from the complex **1**, the key factor with this architecture is the existence of multi-coordinated O atoms from the guest NO₃⁻ ion and the host N atoms, leading to the intermolecular weak O···H–C hydrogen bonding and O···N interaction. They are adequate to achieve directionally controlled aggregation in the solid state.

2.4. The reaction of 2 with KSCN and crystal structures of [Cu(L)(NCS)(CH₃O)]₂ · 2CH₃OH (2A)

In complex **2**, the Cu(II) ion is four-coordinated. Generally, the coordination number of Cu(II) may be four, five or six in complexes and four-coordinated Cu(II) could be considered coordinatively unsaturated metal centers. Thus, we suspect that complex **2** can serve as a precursor complex for new reaction products. When we introduce KSCN to the DMF/methanol mixture solution of **2** at room temperature, as anticipated, the addition reaction of **2** with KSCN yields a new complex **2A**. Single-crystal X-ray analysis reveals **2A** is a neutral binuclear entities and its structure is similar to that of the precursor **2**. In complex **2A**, two Cu(II) atoms still are bridged via two L and two methoxy groups (Fig. 3). The intra-dimeric Cu···Cu distance is 3.023 Å, which is longer than that of complex **2**. But due to the coordination of SCN⁻, Cu(II) becomes five-coordinated and possesses a distorted trigonal bipyramidal environment with two nitrogen atoms (N1 and N6A) from two L and two oxygen atoms (O1 and O1A) from two methoxy groups and one nitrogen atom (N7) from a coordinated NCS⁻ group. Atoms O1A, N6A and N7 occupy the equatorial positions, while atoms N1 and O1 are in the axial positions. Zn–N(L) distances are 1.997(4) and 2.198(4) Å, respectively; Zn–O(CH₃O⁻) bond lengths are 1.879(4) and 1.939(4) Å, respectively; Zn–N(NCS⁻) distance is 2.082(4) Å. There are weak C–H···S interaction and the S···S interaction between L and NCS⁻ groups from two neighboring binuclear

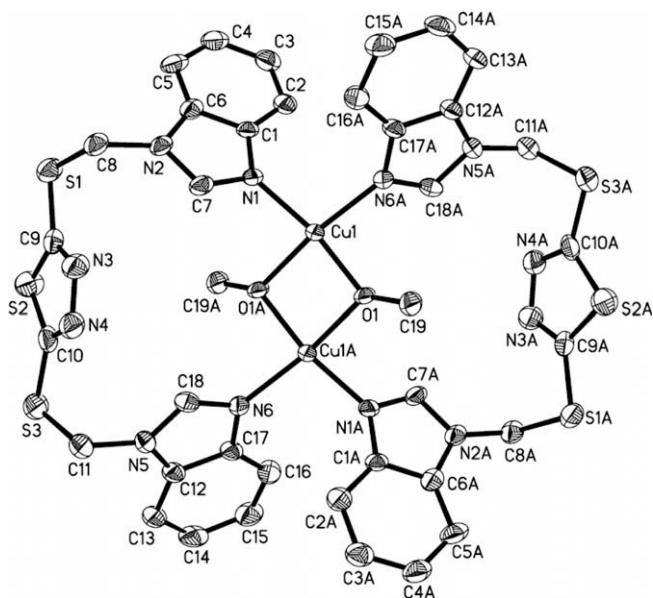**Fig. 2.** ORTEP structure with 30% thermal ellipsoid probability for complex **2** (NO₃⁻, hydrogen atoms and solvent molecules are omitted for clarity).
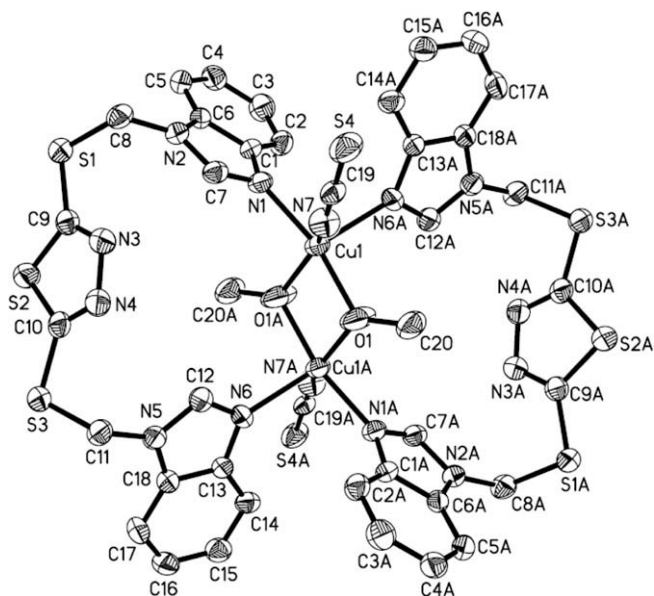
Fig. 3. ORTEP structure with 30% thermal ellipsoid probability for complex **2A**.

molecules, which further assembles into a 1-D chain supramolecular architecture.

2.5. Crystal structures of [Cu(L)(Cl)(N₃)]₂ · 2CH₃OH (3)

Complex **3** is a neutral binuclear molecule which consists of two Cu(II) cations, two L, two azido groups and two chlorine ions (Fig. 4). It features a double u-1,1-azido bridged Cu(II) dimmer. The bond lengths of Cu1–N7 and Cu1–N7A are 1.999(2) and 2.005(2) Å, respectively. In complex **3**, the ligand L adopts the same conformation with complexes **2** and **2A** and bridges two Cu(II) centers. The distances Cu1–N1 and Cu1–N6A are 1.984(2) and 2.010(2) Å, respectively. And the Cu1···Cu1A separation is 3.079 Å. The Cu(II) ions has a distorted penta-coordinated geometry in which the basal plane is composed of the four nitrogen donor atoms. Amongst them two nitrogen atoms are from the bridging azido anions and the other two nitrogen atoms are from L. On the other hand, the fifth coordination site of the square pyramid is occupied by the chlorine ion. The distance Cu1–Cl1 is 2.5423(10) Å. The adjacent binuclear molecules are connected together through intermolecular weak C–H···N hydrogen-bonding interaction, forming a 2-D supramolecular framework.

2.6. The reaction of 3 with Cu(ClO₄)₂ and crystal structures of [Cu(L)(ClO₄)(N₃)]₂ · 2CH₃OH (3A)

In **3**, the five-coordinated Cu(II) could be considered coordinatively unsaturated metal centers. Therefore, it is also expected to display wonderful reactivities and serve as a precursor complex for new reaction products. Attempts to introduce Cu(ClO₄)₂ to the DMF/methanol mixture solution of **3** at room temperature, a new binuclear complex [Cu(L)(ClO₄)(N₃)]₂ · 2CH₃OH (**3A**) is afforded by the anion exchange reaction. X-ray crystallographic study indicates the skeletons of precursor **3** keep unchangeable in **3A** and just the terminal Cl⁻ groups in **3** are completely substituted by the bridging ClO₄⁻ groups (Fig. 5). In **3A**, the intra-dimeric Cu···Cu distance is 2.9418(16) Å, which is shorter than that of complex **3**.

There appears to be no direct hydrogen bonding but the face-to-face π–π stacking interaction with a intermolecular distance of 3.753 Å. This weak stacking interaction is observed between the phenyl ring and the five-numbered ring, which are assembled into
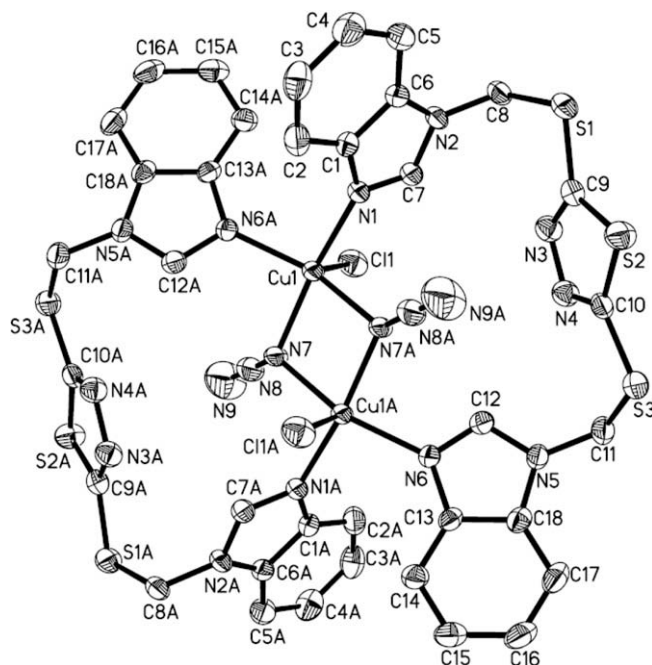

Fig. 4. ORTEP structure with 30% thermal ellipsoid probability for complex **3**.
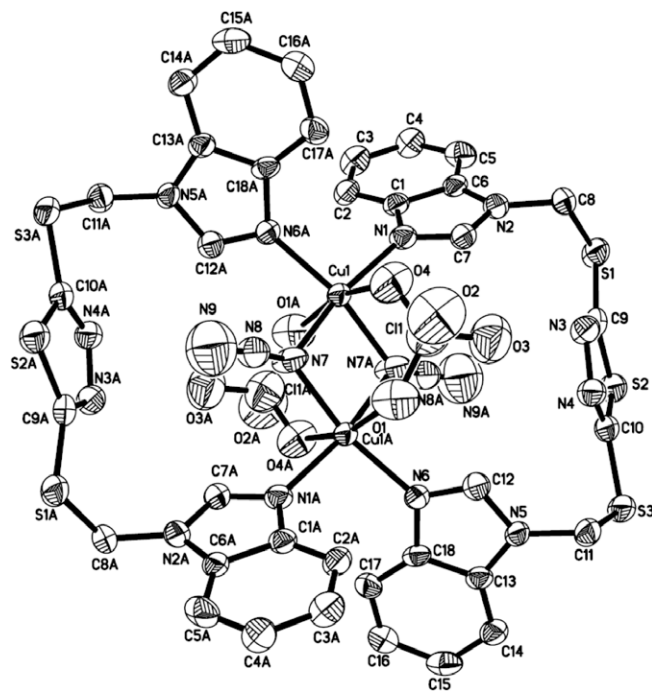
Fig. 5. ORTEP structure with 30% thermal ellipsoid probability for complex **3A**.

a 1-D chain structure. Furthermore, in this chain, every molecule extends to an X-shaped conformation via the head-to-tail face-to-face stacking interaction and thus stabilizes the molecular structure.

2.7. The role of anions in the self-assembly processes

Three Cu(II) coordination complexes **1**, **2** and **3** were synthesized by the self assembly reactions of the flexible ligand bis-(1-benzoimidazolymethylene)-(2,5-thiadiazoly)-disulfide (L) and

Cu(II) salts with different anions, i.e. SO_4^{2-}, NO_3^-, N_3^- and Cl^-. The structures are dependent on the anions. The chelating and bridging SO_4^{2-} anion induced the formation of five-coordinated Cu(II) ions and further assembled to 1-D double-chain chain for **1**. The non-coordinating NO_3^- anion gives rise to the formation of a dimeric structure of **2**. The use of the coordination bridging N_3^- and terminal Cl^- anions result in the formation of a dimeric structure of **3**. From above results, we can conclude that the counteranions in determining the molecular structures play the key role for complexes **1**, **2** and **3**. In fact, the influence of inorganic anions (such as Cl^-, SO_4^{2-}, NO_3^-, etc.) on the structures of complexes has been extensively studied [31–34]. For example, a series of AgX complexes [32] (X = SO_4^{2-}, BF_4^-, ClO_4^-, PF_6^{2-}, $CF_3CO_6^{2-}$ and $CF_3SO_3^-$) have been reported. And the conclusion that the molecular construction via self-assembly is delicately dependent upon the nature of the anions have been drawn. Similar conclusion has also been obtained by Ding et al. [35]. The nature of the anions, especial their coordination modes, are the underlying reason behind the differences in the structures of this series of complexes. This result is consistent with the previous conclusion that counteranions with different coordination modes or abilities can play a key role in crystal engineering [36]. It should be pointed out that the reaction conditions (solvent, temperature, and metal–ligand ratio) are kept constant in these self-assembly processes. Obviously, anions display the key role in tuning the resultant structural topologies. However, for the two new derivative complexes **2A** and **3A** which is obtained by the anion addition and exchange reaction of **2** or **3,** their structural structure keep unchangeable before and after reaction and the new counteranions only bind to the active position of precursor complexes. The results imply that, different from the obvious effects on the structures in the direct self-assembly of the metal and ligand, the change of counteranions has no great impact on the structures in the anion exchange reactions. Generally, the counterions can show different coordination modes in the structure, such as, bridging the metal ions, coordinating with metal ions as terminal coligands, or without coordinating with the metal ions but still having template effects on the structures, etc. [36–38]. Our results also indicate that, in the direct self-assembly progress, even though we only change the counterions, the structures of reaction products are still hard to be controlled. Thus, for the complexes which can not be obtained by the direct self-assembly method, we can attempt to synthesize them by the anion exchange reactions. Some researchers have pointed that the introduction of some simply counterions can produce significant impacts on the properties of compounds [39,40]. As a result, we can tune the properties of complexes by the anion addition and exchange reactions under unchanging the structure skeleton of complexes.

2.8. Catalytic properties of the complexes

The oxidative coupling of 2,6-dimethylphenol (DMP) has received extremely intensive interest because the main product of this reaction, poly(1,4-phenylene ether) (PPE), is a valuable engineering plastic with excellent mechanical properties and chemical resistance [41–45]. In the reaction process, many binuclear copper complexes have been found to be highly active catalysts [46,47]. However, to date, the reaction mechanism for the formation of this important polymer is still not well illustrated. In order to understand the structural and chemical factors that govern the activities of catalysts and searches the more effective catalysts, it is necessary to study the catalytic-structural correlations through examining the effects of coordination environment on the catalytic activities of the copper complexes.

The binuclear copper complexes **2**, **2A**, **3** and **3A** have similar structural frameworks. Thus, in order to investigate the actions of the copper complexes for the formation of DMP, selecting the four complexes as catalysts should be very persuasive. Here, the catalytic activities of these complexes are tested for the oxidative coupling of DMP with H_2O_2 as oxidant and NaOMe as co-catalyst at room temperature. The C–O coupling of DMP yields the linear polymer PPE, the C–C coupling and subsequent oxidation of two DMP units result the by-product diphenoquinone (DPQ).

The yields and selectivity of PPE for the four complexes are shown in Table 1. We find that the catalytic activities of these complexes possess big differences. The bis-μ-alkoxo bridged binuclear copper compound **2** records the high conversion of DMP of 87% with the high selectivity of 91% to PPE. While its derivative compound **2A** with two coordinated thiocyanate ions records the conversion of DMP of 73% with the selectivity of 85% to PPE. The conversion of 67% is obtained with the selectivity of 79% by the use of the bis-μ-azido bridged binuclear copper compound **3**, while its derivative compound **3A** with two bridged ClO_4^- ions is found to be the least active catalyst with only 35% conversion and 72% selectivity. Meantime, we find that the contrasting reaction using $CuCl_2$ or L as catalyst only gives trace amounts of PPE. In addition, we also notice that the $Cu(NO_3)_2$/Meim (Meim = *N*-methyl-imidazole) catalyst which has been used successfully in organic systems, shows a poor result in water with almost no PPE obtained [48]. This suggests that the four complexes have obvious comparative advantage in the aqueous-medium oxidative coupling of DMP.

Since the four complexes have the same main ligand L, the same central metal ion and the similar structural frameworks, we can ascribe the big difference of the activity of the catalysts to the nature of coordinated anions and coordination member of the central metal ion. From previous studies, it has been proposed that the bridged coordination of DMP to dicopper(II) ions to form the active copper species is a key process in the polymerization of DMP to PPE [46–47]. Both of the electrophilicity [49] and coordination environment [50] of the central copper ions in the copper complex have important influences on their catalytic activities in the reaction progress. Obviously, the more electrophilic or the less steric congestive of the copper center is, the more higher the catalytic activity of the complex can be expected. In complex **2**, the coordination number of the copper ion is four. While in complexes **2A**, **3** and **3A**, the coordination numbers of the copper ion are five or six. Compared with complex **2**, the latter three complexes with high coordination number show the bigger steric hindrance, which restrains the substrate to coordinate to the copper(II) ions and forms the proposed dinuclear active species of the polymerization. Especially, in **3A**, the bridged mode of ClO_4^- ions leads to the coor-

Table 1
Oxidative coupling of DMP catalyzed by complexes **2**, **2A**, **3** and **3A**.

Catalysts	Conversion (%)	Yield (%) PPE	Yield (%) DPQ	Selectivity (%) for PPE
2	87	75	7	91
2A	73	57	10	85
3	67	49	13	79
3A	35	21	8	72
CuCl₂	Trace	–	–	–
L	Trace	–	–	–

dination saturation of copper(II) centers, which also prevents strongly the active complex formation between **3A** and DMP. Thus, **3A** shows the worst catalytic activities. In addition, for complexes **2A**, **3** and **3A**, the electron donating effect of the strongly coordinated anions should be another reason for their poor catalytic activities. Our result demonstrates that different coordination counterions in these binuclear copper complexes produce significant impacts on their catalytic properties. Meantime, the result also implies that tuning the properties of complexes by exchanging counteranions should be a feasible method to obtain new materials with desired structures and properties.

3. Experimental

3.1. General information and materials

All chemicals were of reagent-grade quality and were obtained from commercial sources and used without further purification. Elemental analyses (C, H, and N) were carried out on a FLASH EA 1112 analyzer. Infrared spectra data were recorded on a Bruker TENSOR 27 spectrophotometer with KBr pellets in the 400–4000 cm^{-1} region.

3.2. Preparation of bis-(1-benzoimidazolymethylene)-(2,5-thiadiazoly)-disulfide (L)

L was prepared according to the literature method [51]. A mixture of 2,5-dimercapto-thiadiazole (15.2 g, 0.1 mol) and potassium hydroxide (11.2 g, 0.2 mol) was stirred in methanol solution for 15 min. 1-chloridemethylene-benzimidazole (33.2 g, 0.2 mol) was dissolved in 50 ml methanol and was slowly added to the above mixture. The reaction solution was stirred at room temperature for 24 h. The white precipitate was collected and crystallized from ethanol (yield 80%). *Anal.* Calc. for $C_{18}H_{14}N_6S_3$: C, 52.68; H, 3.41; N, 20.49. Found: C, 52.71; H, 3.45; N, 20.42%. IR (cm^{-1}, KBr): 3107m, 2919s, 1624m, 1492m, 1261w, 745m.

3.3. Preparation of {[Cu(SO₄)(L)] · (CH₃OH)}ₙ (**1**)

A methanol solution (4 ml) of L (41 mg, 0.1 mmol) was dropwise added into an aqueous solution (3 ml) of $CuSO_4 \cdot 5H_2O$ (25 mg, 0.1 mmol) to give a clear solution. The resulting solution was allowed to stand in air at room temperature for three weeks, yielding blue crystals (yield 65%) suitable for X-ray diffraction. *Anal.* Calc. for $C_{19}H_{18}CuN_6O_5S_4$: C, 37.87; H, 2.99; N, 13.95. Found: C, 37.95; H, 2.91; N, 13.92%. IR (cm^{-1}, KBr): 3426s, 2367w, 1625m, 1512m, 1391m, 1141s, 748s.

3.4. Preparation of {[Cu(L)(CH₃O)]₂(NO₃)₂} · 2H₂O (**2**)

The procedure was the same as that for **1**, only $Cu(NO_3)_2 \cdot 3H_2O$ instead of $CuSO_4 \cdot 5H_2O$. Yield: 75%. *Anal.* Calc. for $C_{20}H_{21}CuN_7O_5S_3$: C, 40.07; H, 3.50; N, 16.36. Found: C, 40.14; H, 3.48; N, 16.31%. IR (cm^{-1}, KBr): 3428m, 2371s, 1626m, 1384s, 1040m, 748m.

3.5. Preparation of [Cu(L)(NCS)(CH₃O)]₂·2CH₃OH (**2A**)

The crystals of **2** (5.99 mg, 0.01 mmol) were dissolved in DMF solution (3 mL). A methanol solution (6 mL) of KSCN (0.97 mg, 0.01 mmol) was added dropwise to the above solution. The resulting solution was allowed to stand in air at room temperature for three weeks, yielding blue crystals (yield: 62%) suitable for X-ray diffraction. *Anal.* Calc. for $C_{21}H_{21}CuN_7O_2S_4$: C, 42.35; H, 3.53; N, 16.47. Found: C, 42.39; H, 3.58; N, 16.41%. IR (cm^{-1}, KBr): 3429s, 2369w, 2082 m, 1633 m, 1384w, 1191w, 746 m.

3.6. Preparation of [Cu(L)(Cl)(N₃)]₂ · 2CH₃OH (**3**)

An aqueous solution (2 mL) of NaN₃ (6.5 mg, 0.1 mmol) was added into an aqueous solution (1 mL) of CuCl₂ (17 mg, 0.1 mmol), and then a methanol solution (5 mL) of L (41 mg, 0.1 mmol) was slowly diffused into the above mixture. The resultant solution was left at room temperature. Blue crystals (yield 60%) suitable for X-ray diffraction were formed three days later. *Anal.* Calc. for $C_{19}H_{18}ClCuN_9OS_3$: C, 39.07; H, 3.08; N, 21.59. Found: C, 39.14; H, 3.02; N, 21.65%. IR (cm^{-1}, KBr): 3443s, 2364s, 2061s, 1633m, 1509m, 1385w, 1186w.

3.7. Preparation of [Cu(L)(ClO₄)(N₃)]₂ · 2CH₃OH (**3A**)

The crystals of **3** (5.84 mg, 0.01 mmol) were dissolved in DMF solution (3 mL). A methanol solution (6 mL) of $Cu(ClO_4)_2 \cdot 6H_2O$ (2.62 mg, 0.01 mmol) was added dropwise to the above solution. The resulting solution was allowed to stand in air at room temperature for three weeks. Good quality blue crystals were obtained. Yield: 43%. *Anal.* Calc for $C_{21}H_{21}CuN_7O_2S_4$: C, 42.35; H, 3.53; N, 16.47. Found: C, 42.39; H, 3.58; N, 16.41%. IR (cm^{-1}, KBr): 3425s, 2369w, 2069m, 1633m, 1507mm, 746s.

3.8. Crystal structure determination

A crystal suitable for X-ray determination was mounted on a glass fiber. The data of **1** and **2** were collected at room temperature on a Rigaku Saturn 724 CCD with graphite monochromated Mo Kα radiation ($\lambda = 0.71073$ Å). The data of **2A**, **3** and **3A** were performed

Table 2
Crystal data and structure refinement for complexes **1**, **2**, **2A**, **3** and **3A**.

Polymers	**1**	**2**	**2A**	**3**	**3A**
Formula	$C_{19}H_{18}CuN_6O_5S_4$	$C_{20}H_{21}CuN_7O_5S_3$	$C_{21}H_{21}CuN_7O_2S_4$	$C_{38}H_{36}Cl_2Cu_2N_{18}O_2S_6$	$C_{36}H_{28}Cl_2Cu_2N_{18}O_8S_6$
FW	602.17	599.16	595.23	1167.19	1231.10
Crystal system	Triclinic	Triclinic	Triclinic	Monoclinic	Tetragonal
Space group	$P\bar{1}$	$P\bar{1}$	$P\bar{1}$	$P2(1)/n$	$I4(1)/a$
a/(Å)	9.757(2)	9.1770(18)	9.663(4)	12.5158(12)	29.7979(14)
b/(Å)	10.620(2)	11.976(2)	11.930(5)	15.7894(15)	29.7979(14)
c/(Å)	12.297(3)	11.992(2)	12.139(5)	12.8041(12)	11.7053(11)
a/°	87.17(3)	69.59(3)	116.222(4)	90	90
b/°	77.24(3)	87.33(3)	90.868(5)	108.3310(10)	90
g/°	69.65(3)	82.57(3)	93.855(5)	90	90
V/Å³	1164.7(4)	1224.8(4)	1251.0(8)	2401.9(4)	10393.3(12)
Z	2	2	2	2	8
Dc/g cm⁻³	1.717	1.625	1.58	1.614	1.574
$R_1(I > 2\sigma)$	0.0535	0.0806	0.0599	0.0355	0.0862
wR_2 (all date)	0.1294	0.1751	0.1792	0.0902	0.2698
GOF	1.032	0.999	0.896	1.028	1.032

Table 3
Selected bond lengths [Å] and angles [º] for complexes **1**, **2**, **2A**, **3** and **3A**.

Complex **1**					
Cu(1)–O(1)#2	2.258(3)	Cu(1)–O(3)	2.000(3)	Cu(1)–O(4)	1.994(3)
Cu(1)–N(6)#1	1.959(3)	Cu(1)–N(1)	1.986(4)	N(6)#1–Cu(1)–N(1)	96.35(15)
N(6)#1–Cu(1)–O(4)	162.46(14)	N(1)–Cu(1)–O(4)	94.57(14)	N(6)#1–Cu(1)–O(3)	94.99(13)
O(4)–Cu(1)–O(3)	71.06(13)	N(1)–Cu(1)–O(3)	160.87(14)	N(6)#1–Cu(1)–O(1)#2	96.72(14)
N(1)–Cu(1)–O(1)#2	90.04(14)	O(4)–Cu(1)–O(1)#2	96.96(13)	O(3)–Cu(1)–O(1)#2	103.88(13)
Complex 2					
Cu(1)–O(1)	1.885(4)	Cu(1)–O(1)#1	1.925(4)	Cu(1)–N(1)	1.946(5)
Cu(1)–Cu(1)#1	2.8492(19)	Cu(1)–N(6)#1	2.023(5)	O(1)–Cu(1)–O(1)#1	83.22(19)
O(1)–Cu(1)–N(1)	169.5(2)	O(1)#1–Cu(1)–N(1)	87.1(2)	O(1)–Cu(1)–N(6)#1	90.1(2)
O(1)#1–Cu(1)–N(6)#1	167.5(2)	N(1)–Cu(1)–N(6)#1	100.2(2)		
Complex 2A					
Cu(1)–O(1)	1.939(4)	Cu(1)–O(1)#1	1.879(4)	Cu(1)–N(1)	1.997(4)
Cu(1)–N(6)#1	2.198(4)	Cu(1)–N(7)	2.082(4)	O(1)#1–Cu(1)–O(1)	75.30(17)
O(1)#1–Cu(1)–N(1)	93.99(15)	O(1)–Cu(1)–N(1)	166.94(18)	O(1)#1–Cu(1)–N(7)	139.6(2)
O(1)#1–Cu(1)–N(6)#1	94.8(2)	N(1)–Cu(1)–N(6)#1	97.16(15)	N(7)–Cu(1)–N(6)#1	98.27(17)
Complex 3					
Cu(1)–N(1)	1.984(2)	Cu(1)–N(7)	1.999(2)	Cu(1)–N(7)#1	2.005(2)
Cu(1)–Cl(1)	2.5423(10)	Cu(1)–N(6)#1	2.010(2)	N(1)–Cu(1)–N(7)	168.97(10)
N(1)–Cu(1)–N(7)#1	90.76(9)	N(7)–Cu(1)–N(7)#1	79.47(10)	N(1)–Cu(1)–N(6)#1	95.19(9)
N(7)#1–Cu(1)–N(6)#1	154.18(11)	N(7)–Cu(1)–N(6)#1	91.53(10)	N(1)–Cu(1)–Cl(1)	94.11(8)
N(7)–Cu(1)–Cl(1)	92.92(9)	N(7)#1–Cu(1)–Cl(1)	101.93(9)	N(6)#1–Cu(1)–Cl(1)	102.67(8)
Complex 3A					
Cu(1)–N(7)	1.958(6)	Cu(1)–N(7)#1	1.950(6)	Cu(1)–N(6)#1	1.984(6)
Cu(1)–O(1)#1	2.371(11)	Cu(1)–N(1)	1.997(6)	Cu(1)–O(4)	2.332(11)
N(7)#1–Cu(1)–N(1)	90.5(3)	N(7)–Cu(1)–N(1)	167.3(3)	N(6)#1–Cu(1)–N(1)	97.3(2)
N(7)#1–Cu(1)–O(4)	90.4(4)	N(7)–Cu(1)–O(4)	80.2(4)	N(1)–Cu(1)–O(4)	89.3(3)
N(1)–Cu(1)–O(1)#1	99.0(3)	O(4)–Cu(1)–O(1)#1	166.0(3)	N(6)#1–Cu(1)–O(4)	102.2(3)

Symmetry transformations used to generate equivalent atoms in **1**: #1 $x + 1$, y, z; #2 $-x + 1$, $-y$, $-z$; #3 $x - 1$, y, z; #4 x, $y + 1$, z.
Symmetry transformations used to generate equivalent atoms in **2**: #1 $-x + 1$, $-y + 2$, $-z + 1$; #2 $-x + 1$, $-y + 1$, $-z + 1$.
Symmetry transformations used to generate equivalent atoms in **2A**: #1 $-x$, $-y + 1$, $-z + 1$.
Symmetry transformations used to generate equivalent atoms in **3**: #1 $-x + 1$, $-y + 2$, $-z + 2$; #2 $-x + 1$, $-y + 2$, $-z + 1$.
Symmetry transformations used to generate equivalent atoms in **3A**: #1 $-x + 2$, $-y$, $-z + 2$.

at room temperature on a Bruker Aper CCD with graphite monochromated Mo Kα radiation (λ = 0.71073 Å). The structures were solved by direct methods and expanded with Fourier techniques. The non-hydrogen atoms were refined anisotropically. Hydrogen atoms were included but not refined. The final cycle of full-matrix least-squares refinement was based on observed reflections and variable parameters. All calculations were performed with the SHEL-XL-97 crystallographic software package [52]. Table 2 shows crystallographic crystal data and processing parameters for all complexes, and Table 3 list selected bond lengths and bond angles.

3.9. Catalytic experiments

The following is the standard procedure for the polymerization: all crystal complex catalysts (1 mg/FW of **2** = 1.67 × 10^{-3} mmol, 1 mg/FW of **2A** = 1.68 × 10^{-3} mmol, 1 mg/FW of **3** = 1.71 × 10^{-3} mmol and 1 mg/FW of **3A** = 1.62 × 10^{-3} mmol) were powdered to increase the surface area prior to use. Under air, 2,6-dimethylphenol (1 mmol) was dissolved in the 1:1 (v/v, 5 ml) mixture of methanol–toluene in a 10 mL flask, and a 0.5% molar ratio of catalyst/substrate and a 5 M ratio of NaOMe/catalyst were added to above solution with a magnetic stirrer. Then, hydrogen peroxide (30% aqueous solution) was slowly added into the mixture using a syringe pump every 15 min 10 μl for three times to minimize H_2O_2 decomposition. After 2 h, the sample was concentrated in vacuo, and the products were separated by preparative TLC performed on dry silica gel plates with acetic ether–petroleum ether (1:3 v/v) as the developing solvents. PPE and DPQ were collected and dried in vacuo. All reactions were run in duplicate, and the data reported represent the average of these reactions. Poly (phenylene ether) (PPE): ^{1}H NMR: (400 MHz, CDCl$_3$): δ = 2.10 ppm (s, 6H; CH$_3$), δ = 6.45 ppm (s, 2H; H$_{Ar}$); ^{13}C NMR: (100 MHz, CDCl$_3$): δ = 16.8 (CH$_3$), 114.5 (CH), 132.7 (C), 145.6 (C), 154.5 (C) ppm; IR (KBr): 3429(m), 1607(s), 1471(s), 1306(s), 1189(s), 1022(s), 858(m) cm^{-1}.

Appendix A. Supplementary material

CCDC 682728–682732 contain the supplementary crystallographic data for this paper. These data can be obtained free of charge from The Cambridge Crystallographic Data Centre via www.ccdc.cam.ac.uk/data_request/cif. Supplementary data associated with this article can be found, in the online version, at doi:10.1016/j.jorganchem.2009.03.045.

References

[1] X.J. Li, X.Y. Wang, S. Gao, R. Cao, Inorg. Chem. 45 (2006) 1508–1516.
[2] S.R. Batten, R. Robson, Angew. Chem., Int. Ed. 37 (1998) 1460–1494.
[3] P. Dapporto, M. Formica, V. Fusi, M. Micheloni, P. Paoli, R. Pontellini, P. Romani, P. Rossi, Inorg. Chem. 39 (2000) 2156–2163.
[4] J.J. Perry, G.J. McManus, M.J. Zaworotko, Chem. Commun. (2004) 2534–2535.
[5] S. Leininger, B. Olenyuk, P.J. Stang, Chem. Rev. 100 (2000) 853–908.
[6] J.M. Shi, W. Xu, Q.Y. Liu, F.L. Liu, Z.L. Huang, H. Lei, W.T. Yu, Q. Fang, Chem. Commun. (2002) 756–757.
[7] L. Carlucci, G. Ciani, D.M. Proserpio, Coord. Chem. Rev. 246 (2003) 247–289.
[8] S.R. Seidel, P.J. Stang, Acc. Chem. Res. 35 (2002) 972–983.
[9] J. Legros, C. Bolm, Chem. Eur. J. 11 (2005) 1086–1092.
[10] J.P. Zhang, Y.Y. Lin, X.C. Huang, X.M. Chen, J. Am. Chem. Soc. 127 (2005) 5495–5506.
[11] W.B. Connick, J. Am. Chem. Soc. 130 (2008) 4205.
[12] S.E. Castillo-Blum, N. Barba-Behrens, Coord. Chem. Rev. 196 (2000) 3–30.
[13] H. Jude, J.A.K. Bauer, W.B. Connick, Inorg. Chem. 44 (2005) 1211–1220.
[14] W.Y. Sun, T. Kusukawa, M. Fujita, J. Am. Chem. Soc. 124 (2002) 11570–11571.
[15] R. Schneider, M.W. Hosseini, J.M. Planeix, A.D. Cian, J. Fischer, Chem. Commun. (1998) 1625–1626.

[16] J.S. Hall, J.G. Loeb, K.H. Shimizu, G.P.A. Yap, Angew. Chem., Int. Ed. 37 (1998) 121–123.
[17] R.D. Schnebeck, E. Freisinger, B. Lippert, Angew. Chem., Int. Ed. 38 (1999) 168–171.
[18] R.H. Wang, D.Q. Yuan, F.L. Jiang, L. Han, Y.Q. Gong, M.C. Hong, Cryst. Growth Des. 6 (2006) 1351–1360.
[19] X.P. Zhou, X.J. Zhang, S.H. Lin, D. Li, Cryst. Growth Des. 7 (2007) 485–487.
[20] O.S. Jung, S.H. Park, K.M. Kim, H.G. Jang, Inorg. Chem. 37 (1998) 5781–5785.
[21] M.A. Withersby, A.J. Blake, N.R. Champness, P.A. Cooke, P. Hubberstey, W.S. Li, M. Schröder, Inorg. Chem. 38 (1999) 2259–2266.
[22] H.B. Chen, H. Zhang, J.M. Yang, Z.H. Zhou, Polyhedron 23 (2004) 987–991.
[23] M. Du, Y.M. Guo, S.T. Chen, X.H. Bu, Inorg. Chem. 43 (2004) 1287–1293.
[24] O.S. Jung, Y.J. Kim, Y.A. Lee, H.K. Chae, H.G. Jang, J. Hong, Inorg. Chem. 40 (2001) 2105–2110.
[25] G. Yang, R.G. Raptis, Chem. Commun. (2004) 2058–2059.
[26] C.Y. Su, B.S. Kang, Q.C. Yang, T.C.W. Mak, J. Chem. Soc., Dalton Trans. (2000) 1857–1862.
[27] M.S. Lah, H. Chun, Inorg. Chem. 36 (1997) 1782–1785.
[28] D. Moon, M.S. Lah, R.E.D. Sesto, J.S. Miller, Inorg. Chem. 41 (2002) 4708–4714.
[29] C.J. Matthews, V. Broughton, G. Bernardinelli, X. Melich, G. Brand, A.C. Willis, A.F. Williams, New J. Chem. 27 (2003) 354–358.
[30] R.P. John, M. Park, D. Moon, K. Lee, S. Hong, Y. Zou, C.S. Hong, M.S. Lah, J. Am. Chem. Soc. 129 (2007) 14142.
[31] B.L. Schottel, H.T. Chifotides, M. Shatruk, A. Chouai, L.M. Perez, J. Bacsa, K.R. Dunbar, J. Am. Chem. Soc. 128 (2006) 5895–5912.
[32] O.S. Jung, Y.J. Kim, Y.A. Lee, K.M. Park, S.S. Lee, Inorg. Chem. 42 (2003) 844–850.
[33] B.L. Li, Y.F. Peng, B.Z. Li, Y. Zhang, Chem. Commun. (2005) 2333–2335.
[34] N. Schultheiss, D.R. Powell, E. Bosch, Inorg. Chem. 42 (2003) 5304–5310.
[35] J.G. Ding, X.G. Liu, B.L. Li, L.Y. Wang, Y. Zhang, Inorg. Chem. Commun. 11 (2008) 1079–1081.
[36] G.Q. Zhang, G.Q. Yang, J.S. Ma, Cryst. Growth Des. 6 (2006) 1897–1902.
[37] M.O. Awaleh, A. Badia, F. Brisse, Cryst. Growth Des. 6 (2006) 2674–2685.
[38] D.L. Reger, R.F. Semeniuc, V. Rassolov, M.D. Smith, Inorg. Chem. 43 (2004) 537–554.
[39] J. Ribas, A. Escuer, M. Monfort, R. Vicente, R. Cortés, L. Lezama, T. Rojo, Coord. Chem. Rev. 193–195 (1999) 1027–1068.
[40] W. Zhao, Y. Song, T. Okamura, J. Fan, W.Y. Sun, N. Ueyama, Inorg. Chem. 44 (2005) 3330–3336.
[41] A.S. Hay, H.S. Stafford, G.F. Endres, J.W. Eustance, J. Am. Chem. Soc. 81 (1959) 6335–6336.
[42] P.J. Baesjou, W.L. Driessen, G. Challa, J. Reedijk, J. Mol. Catal. A 135 (1998) 273–283.
[43] P.J. Baesjou, W.L. Driessen, G. Challa, J. Reedijk, J. Am. Chem. Soc. 119 (1997) 12590–12594.
[44] K. Oyaizu, Y. Kumaki, K. Saito, E. Tuschida, Macromolecules 33 (2000) 5766–5769.
[45] S. Gupta, J.A.P.P. Van Dijk, P. Gamez, G. Challa, J. Reedijk, Appl. Catal. A 319 (2007) 163–170.
[46] J. Gao, J. Reibenspies, A.E. Martell, Inorg. Chim. Acta 338 (2002) 157.
[47] P.J. Saesjou, W.L. Driessen, G. Challa, J. Reedijk, J. Mol. Catal. A 110 (1996) 195–210.
[48] P. Gamez, J.A.P.P. van Dijk, W.L. Driessen, G. Challa, J. Reedijk, Adv. Synth. Catal. 344 (2002) 890–893.
[49] P.G. Aubel, S.S. Khokhar, W.L. Driessen, G. Challa, J. Reedijk, J. Mol. Catal. A 175 (2001) 27–31.
[50] B. Xiao, H.W. Hou, Y.T. Fan, J. Organomet. Chem. 692 (2007) 2014–2020.
[51] D.Q. Zhang, L.X. Gao, G.D. Zhou, Appl. Surf. Sci. 225 (2004) 287–293.
[52] G.M. Sheldrick, SHELXTL-97, Program for Refining Crystal Structure Refinement, University of Göttingen, Germany, 1997.